Segmenting Clustered Nuclei Using *H*-minima Transform-Based Marker Extraction and Contour Parameterization

Chanho Jung and Changick Kim*

***Abstract*—In this letter, we present a novel watershed-based method for segmentation of cervical and breast cell images. We formulate the segmentation of clustered nuclei as an optimization problem. A hypothesis concerning the nuclei, which involves *a priori* knowledge with respect to the shape of nuclei, is tested to solve the optimization problem. We first apply the distance transform to the clustered nuclei. A marker extraction scheme based on the *H*-minima transform is introduced to obtain the optimal segmentation result from the distance map. In order to estimate the optimal *h*-value, a size-invariant segmentation distortion evaluation function is defined based on the fitting residuals between the segmented region boundaries and fitted models. Ellipsoidal modeling of contours is introduced to adjust nuclei contours for more effective analysis. Experiments on a variety of real microscopic cell images show that the proposed method yields more accurate segmentation results than the state-of-the-art watershed-based methods.**

***Index Terms*—Cell image segmentation, contour parameterization, *H*-minima transform, marker extraction, watershed-based segmentation.**

I. Introduction

In RECENT years, a number of automated microscopic cellular image analysis techniques has been introduced [1]–[4]. Especially, there have been several approaches to segmenting the nuclei in the literature and most of them have been performed manually or in a semiautomatic manner to obtain more accurate segmentation results [5]. However, the user-interaction hinders the automated cell image analysis [5], [6]. Therefore, developing a sophisticated and unsupervised nuclei segmentation method is necessary to assure the success of the automatic cell image analysis.

One of the main factors, which makes it hard to accurately segment the nuclei, is the existence of clustered nuclei in the cell images [5]–[7]. The watershed algorithm is one of the most widely used segmentation techniques for nuclei extraction [6].

Manuscript received April 13, 2010; revised June 17, 2010; accepted July 6, 2010. Date of publication July 23, 2010; date of current version September 15, 2010. This work was supported by the Ministry of Knowledge Economy (MKE), Korea, under the Information Technology Research Center (ITRC) support program supervised by the National IT Industry Promotion Agency (NIPA) [NIPA-2010-(C1090-1011-0003)]. *Asterisk indicates corresponding author.*

C. Jung is with the Department of Electrical Engineering, Korea Advanced Institute of Science and Technology, Daejeon 305-732, Korea (e-mail: peterjung@kaist.ac.kr).

*C. Kim is with the Department of Electrical Engineering, Korea Advanced Institute of Science and Technology, Daejeon 305-732, Korea (e-mail: cikim@ee.kaist.ac.kr).

Color versions of one or more of the figures in this paper are available online at http://ieeexplore.ieee.org

Digital Object Identifier 10.1109/TBME.2010.2060336

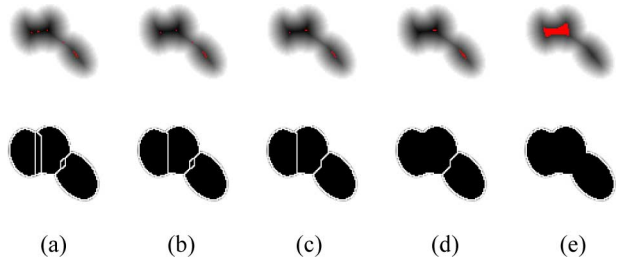

Fig. 1. Regional minima marked in red (upper row) and watershed segmentation results with several h-values: (a) $h = 0$, (b) $h = 1$, (c) $h = 2$, (d) $h = 5$, and (e) $h = 47$.

However, watershed usually yields oversegmentation since regional minima or ultimate eroded points are employed for segmenting nuclei directly. This is because it is difficult to have one-to-one correspondence between regional minima and nuclei. In addition, it becomes worse when the nuclei are clustered. To handle the oversegmentation problem, region merging and marker-controlled watershed techniques have been reported in the literature [5], [6]. The region merging techniques are highly sensitive to the sizes of nuclei. The marker-controlled watershed schemes formulate the segmentation as a marker extraction problem. In the marker-controlled watershed methods, nuclei should be initially represented by the markers appropriately [5], [6]. Thus, the step for elimination of spurious markers that result in oversegmentation of nuclei needs to be employed in the marker-controlled watershed. Meanwhile, mathematical morphology has been involved to obtain the markers accurately [6]. In [6], a maker detection technique based on condition erosion has been introduced. However, the segmentation results tend to rely on incorporated morphological structuring elements and erosion thresholds.

The *H*-minima or *H*-maxima transform is a powerful mathematical tool to suppress undesired minima or maxima [5], [8]–[10]. Performing the *H*-minima transform on the inverse distance image can effectively decrease oversegmentation. On the other hand, the *H*-maxima transform is applied to the distance image. Let g denote the inverse distance map of clustered nuclei. The *H*-minima transform [10] is performed by

$$H_h(g) = R_g^{\varepsilon}(g + h) \tag{1}$$

where h represents the given depth. In (1), R and ε represent the reconstruction and erosion operators, respectively. By using the *H*-minima transform, all minima whose depth is lower than or equal to the given *h*-value are suppressed. Fig. 1 shows regional

minima and corresponding watershed segmentation results from a synthetic clustered nuclei with different *h*-values adopted. As shown in Fig. 1, the *h*-value has a direct influence on the number of segmented regions. The larger the *h*-value is, the fewer the numbers of the segmented regions. In [8] and [9], the *H*-maxima transform has been employed to segment clustered nuclei. However, empirical selection of the *h*-value often makes robust segmentation difficult [8], [9]. Cheng and Rajapakse [5] proposed a marker-controlled watershed technique using the *H*-minima transform. Since the parameters directly related to the *h*-value are applied identically to all clustered nuclei regardless of the nuclei size in [5], the number of nuclei cannot be determined adaptively to the clustered nuclei.

The aim of this letter is to present a fully automated method for segmenting human cervical and breast cell images. In this letter, the segmentation of clustered nuclei is treated as an optimization problem in the watershed-based framework. Typically, the segmentation performance can be extremely improved when *a priori* knowledge of the nuclei is employed [11], [12]. In our study, a hypothesis concerning the nuclei is taken into account within the framework. Since clustered nuclei often contain occlusions, it is reasonable to exploit the occlusion characteristics of the clustered nuclei for solving the optimization problem. We introduce a size-invariant segmentation distortion evaluation function to estimate the optimal *h*-value. Before the optimal *h*-value is estimated, opening-by-reconstruction and closing-by-reconstruction are consecutively applied to eliminate noise without changing the shape of clustered nuclei. In order to compute the distance transform, adaptive thresholding [13] is carried out on the sequentially filtered image. After the distance image is inverted, the inverse distance map is normalized to reduce the influence of the size of clustered nuclei.

II. Proposed Method

In order to estimate the optimal *h*-value in the watershed-based framework, the hypothesis that a nucleus can be described as an ellipsoidal model is tested since the cervical and breast cells usually have ellipse-like shaped boundaries [11], [12]. However, it is noted that the whole boundaries of each nucleus may not be obtained when nuclei are clustered. In other words, what we can observe are the partial boundaries due to occlusion caused by nuclei clustering. Note that this also happens when the nuclei are oversegmented. Thus, we can categorize the nuclei boundaries into two groups: *partial original boundaries* and *boundaries due to clustering or oversegmentation*. Fig. 2 describes the occlusion characteristics of clustered nuclei and categorization of nucleus boundaries.

By employing the occlusion characteristics of clustered nuclei, the marker extraction scheme based on the *H*-minima transform learns the optimal *h*-value by repeatedly evaluating segmentation quality since the watershed transform is controlled by the *h*-value. Specifically, while increasing the depth until the number of regional minima equals one starting from a quite large number, we assess the segmentation quality by using a distortion evaluation function

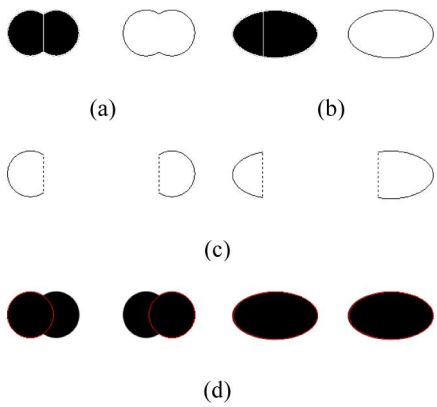

Fig. 2. Occlusion characteristic of clustered nuclei and categorization of nucleus boundaries: synthetic segmentation results and boundaries, which touch background, of (a) clustered and (b) oversegmented nuclei. (c) *partial original boundaries,* which touch background (solid lines) and *boundaries due to clustering or oversegmentation,* which do not touch background (dotted lines), and (d) nucleus modeling results marked in red, obtained from partial original boundaries.

$$S(w_h) = \frac{1}{m}\sum_{i=1}^{m} \mathrm{AFR}(w_{h,i}) \tag{2}$$

where w_h and $w_{h,i}$ denote the segmentation result controlled by h and the ith nucleus of w_h, respectively. m denotes the total number of nuclei in w_h. As we can see in (2), we assume that each nucleus has its own segmentation distortion value, which we call the averaged fitting residual (AFR) and is defined in (4), and the values from all nuclei are averaged to obtain $S(w_h)$. Since we know the partial original boundaries of each nucleus, it is possible to mathematically represent each nucleus using the corresponding elliptical model. Let (u, v) be a point on the partial original boundary. An ellipsoid can be described as an implicit second-order polynomial

$$F(u, v) = au^2 + buv + cv^2 + du + ev + f = 0 \tag{3}$$

where a, b, c, d, e, and f denote the ellipse coefficients. By using the direct least square fitting algorithm [14], the optimal ellipse parameters are estimated. Fig. 2(d) shows ellipsoidal modeling of nucleus computed from the partial original boundaries. Let $F_{h,i}$ denote the ellipsoidal model obtained from $w_{h,i}$ by using (3). $\mathrm{AFR}(w_{h,i})$ is defined as an average of fitting residuals as follows:

$$\mathrm{AFR}(w_{h,i}) = \frac{1}{n_{h,i}}\sum_{j=1}^{n_{h,i}} r(\mathbf{b}_{h,i,j}, F_{h,i}) \tag{4}$$

where $n_{h,i}$ and $\mathbf{b}_{h,i,j}$ represent the number of boundary points and jth boundary point on $w_{h,i}$, respectively, and $r(\mathbf{b}_{h,i,j}, F_{h,i})$ represents the distance from $\mathbf{b}_{h,i,j}$ to the closest point on $F_{h,i}$. Meanwhile, the direct use of $r(\mathbf{b}_{h,i,j}, F_{h,i})$ is not appropriate as a measure of fitting residual, since nuclei have different sizes. Therefore, to make fair evaluations of the residual, the affine transform is employed to convert the ellipsoidal models to the

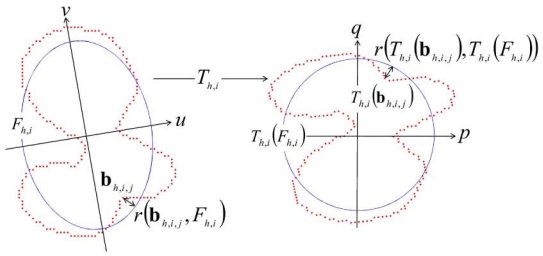

Fig. 3. Affine transform of ellipsoidal model to unit circle.

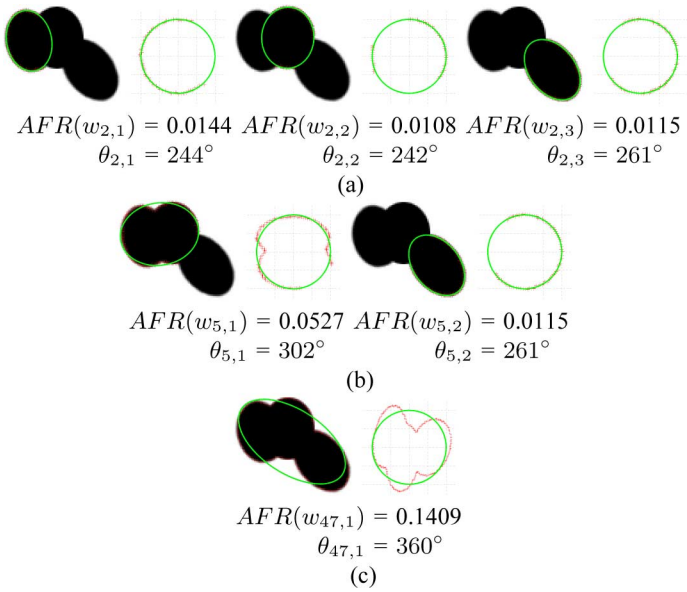

Fig. 4. Estimation of segmentation distortion evaluation functions by measuring fitting residual: (a) $S(w_2) = 0.0122$, (b) $S(w_5) = 0.0321$, and (c) $S(w_{47}) = 0.1409$. Note that the segmentation distortion in (a) is lowest compared to those in (b) and (c). Thus, three nuclei are estimated to exist. (a) case 1: three nuclei segmented with $h = 2$ ($\min(\theta_{2,i}) = 242°$). (b) case 2: two nuclei segmented with $h = 5$ ($\min(\theta_{5,i}) = 261°$). (c) case 3: a nucleus segmented with $h = 47$ ($\min(\theta_{47,i}) = 360°$).

unit circle. Fig. 3 shows the process of the affine transform to the unit circle. By transforming all ellipsoidal models to identical unit circle, r becomes independent of the ellipsoidal parameters. Let $T_{h,i}$ denotes the transform operator. Then, in (4), $r(\mathbf{b}_{h,i,j}, F_{h,i})$ should be replaced by $r(T_{h,i}(\mathbf{b}_{h,i,j}), T_{h,i}(F_{h,i}))$. Finally, the optimal *h*-value can be learned by minimizing the segmentation distortion evaluation function. Fig. 4 shows the segmentation distortion evaluation results with several *h*-values for the synthetic clustered nuclei used in Fig. 1. As shown in the figure, the segmentation distortion evaluation function is minimized when m equals three (i.e., $c = 3$, where c denotes the estimated total number of nuclei). The overall marker extraction procedure based on the *H*-minima transform can be summarized as follows:

In the marker extraction procedure based on the *H*-minima transform, we obtain the initial number of regional minima from

1: **H-minima Transform Based Marker Extraction**:
2: $m \leftarrow$ # initial regional minima
3: $S_{\min} \leftarrow \infty$
4: $h \leftarrow 0$
5: **while** $m > 0$ **do**
6: **repeat**
7: $h \leftarrow h + 1$
8: evaluate $H_h(g)$
9: **until** # regional minima for $H_h(g) \leq m$
10: **if** # regional minima for $H_h(g) = m$ **then**
11: perform watershed on $H_h(g)$
12: **if** $\min(\theta_{h,i}) > \pi + 2\omega$ (see Fig. 4, Fig. 5, and Fig. 6) **then**
13: estimate segmentation distortion evaluation function $S(w_h)$
14: **if** $S(w_h) < S_{\min}$ **then**
15: $S_{\min} = S(w_h)$, $c = m$
16: **end if**
17: **end if**
18: **end if**
19: $m \leftarrow m - 1$
20: **end while**

the normalized inverse distance image of clustered nuclei. Note that line 12 is added to identify oversegmentation before estimating the segmentation distortion evaluation function $S(w_h)$. The *h*-value increases until the criterion in line 12 is satisfied. Once no oversegmentation is detected, the segmentation distortion evaluation function is computed. Fig. 5 shows the proposed scheme to identify oversegmentation. In the scheme, the characteristics of transformed partial original boundaries, obtained from the boundary categorization, provide important clues on how to identify oversegmentation. In Fig. 5, the transformed partial original boundaries of clustered and oversegmented nuclei are compared. Let $\theta_{h,i}$ be the outer angle between vectors $\overrightarrow{T_{h,i}(\mathbf{c}_{h,i})T_{h,i}(\mathbf{b}_{h,i,1})}$ and $\overrightarrow{T_{h,i}(\mathbf{c}_{h,i})T_{h,i}(\mathbf{b}_{h,i,n_{h,i}})}$, where $\mathbf{c}_{h,i}$ represents the center of $F_{h,i}$. When a nucleus is not overlapped to other nuclei nor oversegmented, θ of the nucleus is 2π. However, as shown in Fig. 5(a), the outer angles of clustered nuclei are in the range $(\pi, 2\pi)$ due to occlusion [see also Figs. 4(a) and 6(c)]. In other words, this is because the center $\mathbf{c}$ of a nucleus does not belong with the other regions in the clustered nuclei, as shown in Fig. 5(a), even though the occlusion is extremely severe. On the other hand, at least one outer angle of oversegmented nuclei cannot be larger than π, since the sum of outer angles for the oversegmented nuclei becomes 2π, as shown in Fig. 5(b) (i.e., $\theta_{h,1} + \theta_{h,2} = 2\pi$). In addition, it is noted that the tiny regions, which are fully or mostly surrounded by other regions due to oversegmentation, have the outer angles much less than π [see Fig. 6(b)]. Therefore, the criterion to exclude the oversegmented cases is defined as follows:

$$\min(\theta_{h,i}) > \pi + 2\omega, 1 \leq i \leq m \tag{5}$$

where ω represents an angular margin, which is to take the fitting error into account. If the condition in (5) is not satisfied, the *h*-value is increased and new segmentation results are obtained until (5) is satisfied. For example, the minimum outer angle of synthetic clustered nuclei in Fig. 1 is zero when the *h*-value is 0 or 1, as shown in Fig. 1(a) and (b) (i.e., $\min(\theta_{0,i}) = 0°$

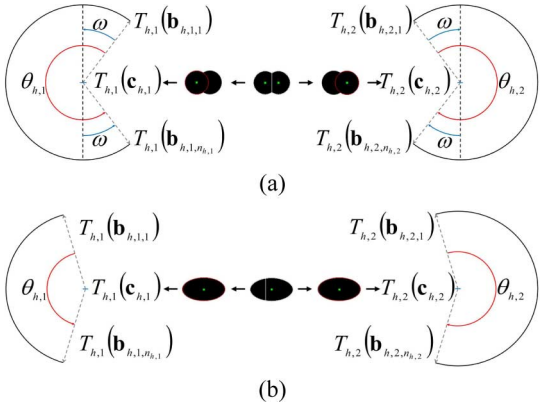

Fig. 5. Finding oversegmentation by using the outer angle $\theta_{h,i}$: (a) $\theta_{h,i}$ of clustered nuclei and (b) $\theta_{h,i}$ of oversegmented nuclei. Note that $\mathbf{c}_{h,1}$ and $\mathbf{c}_{h,2}$ are marked in green.

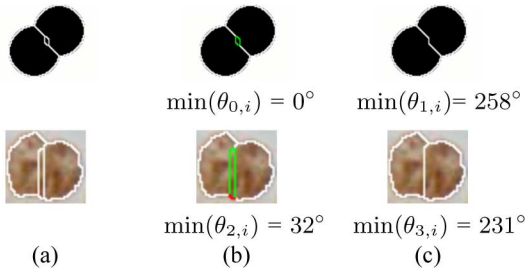

Fig. 6. Estimation of outer angles: (a) watershed segmentation results with $h = 0$ (top) and $h = 2$ (bottom), (b) *partial original boundaries* (marked in red) and *boundaries due to oversegmentation* (marked in green) of regions result from oversegmentation in (a), and (c) watershed segmentation results when *h*-values are increased to $h = 1$ (top) and $h = 3$ (bottom), so that the condition in (5) is satisfied. Note that minimum outer angle of (top) clustered nuclei in (b) is zero since they have a region without partial original boundary.

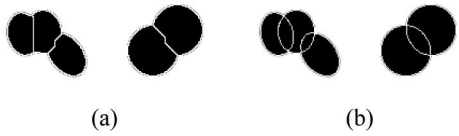

Fig. 7. Contour parameterization: (a) contours by the watershed and (b) contours adjusted by the contour parameterization.

and $\min(\theta_{1,i}) = 0°$). On the other hand, the condition in (5) is satisfied when the *h*-value is larger than 1, as shown in Fig. 4.

The ellipsoidal modeling of the nucleus employed to find the optimal *h*-value in this section is also useful in that the modeling or the contour parameterization facilitates the quantitative analysis of cell images. Note that the watershed segmentation technique usually yields jagged contours [5]. The jagged contour problem by the watershed can be alleviated since the nuclei are described by the parameterized ellipsoidal models. In the framework, we assume that all of the parameterized ellipsoidal models are mutually independent. Thus, the regions of parameterized ellipsoidal models can be overlapped. Fig. 7 shows the comparison of extracted contours. As shown in the figure, our contour parameterization effectively adjusts nuclei contours without the jaggedness.

TABLE 1
COMPARISON OF SEGMENTATION PERFORMANCE FOR CLUSTERED NUCLEI ON SPECIMENS OF CERVICAL CELLS AND MAMMARY INVASIVE DUCTAL CARCINOMAS

		correctly segmented	over-segmented	under-segmented
classical watershed		51.02% (68.10)%	48.47% (31.77)%	0.51% (0.13)%
condition erosion [6]		61.22% (88.28)%	1.02% (2.08)%	37.76% (9.64)%
shape marker [5]		72.45% (91.01)%	15.82% (6.00)%	11.73% (2.99)%
proposed	$\omega = \pi/18$	95.41% (95.96)%	3.06% (3.65)%	1.53% (0.39)%
	$\omega = \pi/12$	96.43% (96.74)%	1.02% (2.61)%	2.55% (0.65)%
	$\omega = \pi/9$	93.37% (96.49)%	0.51% (1.95)%	6.12% (1.56)%

III. RESULTS AND CONCLUSION

In order to evaluate the performance of the proposed method, real microscopic cell images are used. A number of specimens containing cervical cells and mammary invasive ductal carcinomas taken by a light microscope with 40X objective are demonstrated. The Papanicolaou technique is used to stain the specimens of cervical cells. The specimens of mammary invasive ductal carcinomas are stained by immunohistochemistry for the p53 protein and estrogen receptor. The segmentation results by the proposed method are compared with ones from the state-of-the-art watershed-based segmentation techniques, such as the classical watershed, condition erosion [6], and shape marker [5]. The effectiveness of ellipsoidal modeling of nucleus contours is demonstrated on several clustered nuclei. In our study, the angular margin ω is empirically set to $\pi/12$, which provides the best segmentation performance throughout tests.

Table I shows the comparison of segmentation performance for 932 clustered nuclei on 87 microscopic cell images of size 1392×1040. The segmentation results are categorized into three groups: 1) correctly segmented, 2) oversegmented, and 3) undersegmented [5], [6]. To study the sensitivity of the proposed segmentation method to the angular margin, the segmentation is performed by varying the angular margin. As shown in Table I, the proposed algorithm provides the best segmentation performance when the angular margin is set to $\pi/12$. It is also shown that the proposed method is robust and not very sensitive to the variation of angular margins. Meanwhile, in Table I, the comparison of segmentation performance for 5762 nuclei including the aforementioned 932 clustered nuclei on the dataset, which are specimens of cervical cells and mammary invasive ductal carcinomas, is illustrated in bottom parentheses. As shown in the table, the proposed method achieves improvements by 45.41%, 35.21%, and 23.98% with respect to the classical watershed, condition erosion, and shape marker schemes in terms of separation accuracy on 932 clustered nuclei, respectively, when the angular margin is $\pi/12$. It should be noted that, as shown in Table I, the success of nuclei segmentation is highly dependent on the segmentation accuracy on the clustered nuclei. Figs. 8 and 9 show several segmentation results by the proposed scheme and the state-of-the-art watershed-based segmentation methods

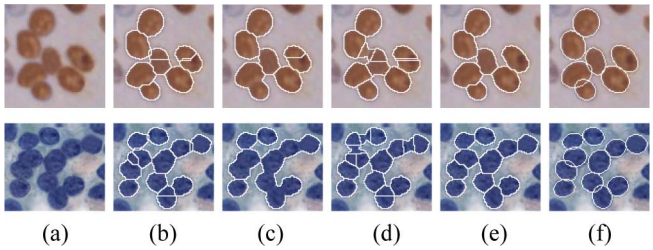

Fig. 8. (a) Original image, segmentation results by (b) classical watershed, (c) condition erosion [6], (d) shape marker [5], (e) proposed method, and (f) contour adjustment by the proposed parameterization method.

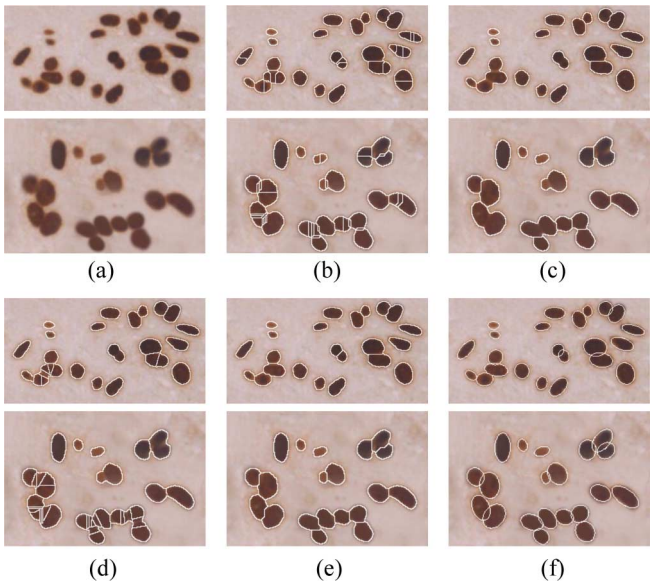

Fig. 9. (a) Original image, segmentation results by (b) classical watershed, (c) condition erosion [6], (d) shape marker [5], (e) proposed method, and (f) contour adjustment by the proposed parameterization method.

on specimens of cervical cells and mammary invasive ductal carcinomas. As we can see in the figures, the proposed method outperforms the conventional approaches. Moreover, it is further turned out that the jaggedness problem is efficiently resolved by the proposed contour adjustment.

In this letter, we have proposed a fully automated watershed-based nuclei segmentation technique. The proposed method can be directly extended to a cell image segmentation system for human body cells, since most cells, such as hypothyroid and intestine cells as well as cervical and breast cells, in the human body usually have ellipse-like boundaries [11]. Experimental results presented in this section prove that the proposed scheme performs better than the state-of-the-art watershed-based methods. Currently, our implementation on Intel Core2 Duo 3 GHz PC takes 1.34 s/image, on average.

REFERENCES

[1] X. Zhou, F. Li, J. Yan, and S. T. C. Wong, "A novel cell segmentation method and cell phase identification using markov model," *IEEE Trans. Info. Tech. Biomed.*, vol. 13, no. 2, pp. 152–157, Mar. 2009.

[2] L. Yang, P. Meer, and D. J. Foran, "Unsupervised segmentation based on robust estimation and color active contour models," *IEEE Trans. Inf. Technol. Biomed.*, vol. 9, no. 3, pp. 475–486, Sep. 2005.

[3] E. A. Carpenter, R. T. Jones, R. M. Lamprecht, C. Clarke, H. I. Kang, O. Friman, A. D. Guertin, and H. J. Chang, "Cellprofiler: Image analysis software for identifying and quantifying cell phenotypes," *Genome Biol.*, vol. 7, no. 10, p. R100, 2006.

[4] M. N. Gurcan, T. Pan, H. Shimada, and J. Saltz, "Image analysis for neuroblastoma classification: Segmentation of cell nuclei," in *Proc. IEEE Ann. Int. Conf. Eng. Med. Biol. Soc.*, 2006, pp. 4844–4847.

[5] J. Cheng and J. C. Rajapakse, "Segmentation of clustered nuclei with shape markers and marking function," *IEEE Trans. Bio. Eng.*, vol. 56, no. 3, pp. 741–748, Mar. 2009.

[6] X. Yang, H. Li, and X. Zhou, "Nuclei segmentation using marker-controlled watershed, tracking using mean-shift, and Kalman filter in time-lapse microscopy," *IEEE Trans. Ciruits Syst. I: Reg. Papers*, vol. 53, no. 11, pp. 2405–2414, Nov. 2006.

[7] F. Cloppet and A. Boucher, "Segmentation of overlapping/aggregating nuclei cells in biological images," in *Proc. IEEE Int. Conf. Pat. Rec.*, 2008, pp. 1–4.

[8] F. Raimondo, M. A. Gavrielides, G. Karayannopoulou, K. Lyroudia, I. Pitas, and I. Kostopoulos, "Automated evaluation of her-2/neu status in breast tissue from fluorescent in situ hybridization images," *IEEE Trans. Imag. Process.*, vol. 14, no. 9, pp. 1288–1299, Sep. 2005.

[9] H. Masmoudi, S. M. Hewitt, N. Petrick, K. J. Myers, and M. A. Gavrielides, "Automated quantitative assessment of her-2/neu immunohistochemical expression in breast cancer," *IEEE Trans. Med. Imag.*, vol. 28, no. 6, pp. 916–925, Jun. 2009.

[10] P. Soille, *Morphological Image Analysis: Principles and Applications*. Berlin, Germany: Springer-Verlag, 1999.

[11] T. Jiang, F. Yang, Y. Fan, and D. J. Evans, "A parallel genetic algorithm for cell image segmentation," *Elec. Notes Theo. Comp. Sci.*, vol. 46, pp. 214–224, 2001.

[12] H.-S. Wu, J. Barba, and J. Gil, "A parametric fitting algorithm for segmentation of cell images," *IEEE Trans. Biomed. Eng.*, vol. 45, no. 3, pp. 400–407, Mar. 1998.

[13] N. Otsu, "A threshold selection method from gray-level histograms," *IEEE Trans. Syst., Man, Cybern.*, vol. SMC-9, no. 1, pp. 62–66, Jan. 1979.

[14] A. Fitzgibbon, M. Pilu, and R. B. Fisher, "Direct least square fitting of ellipses," *IEEE Trans. Patter Anal. Mach. Intell.*, vol. 21, no. 5, pp. 476–480, May 1999.